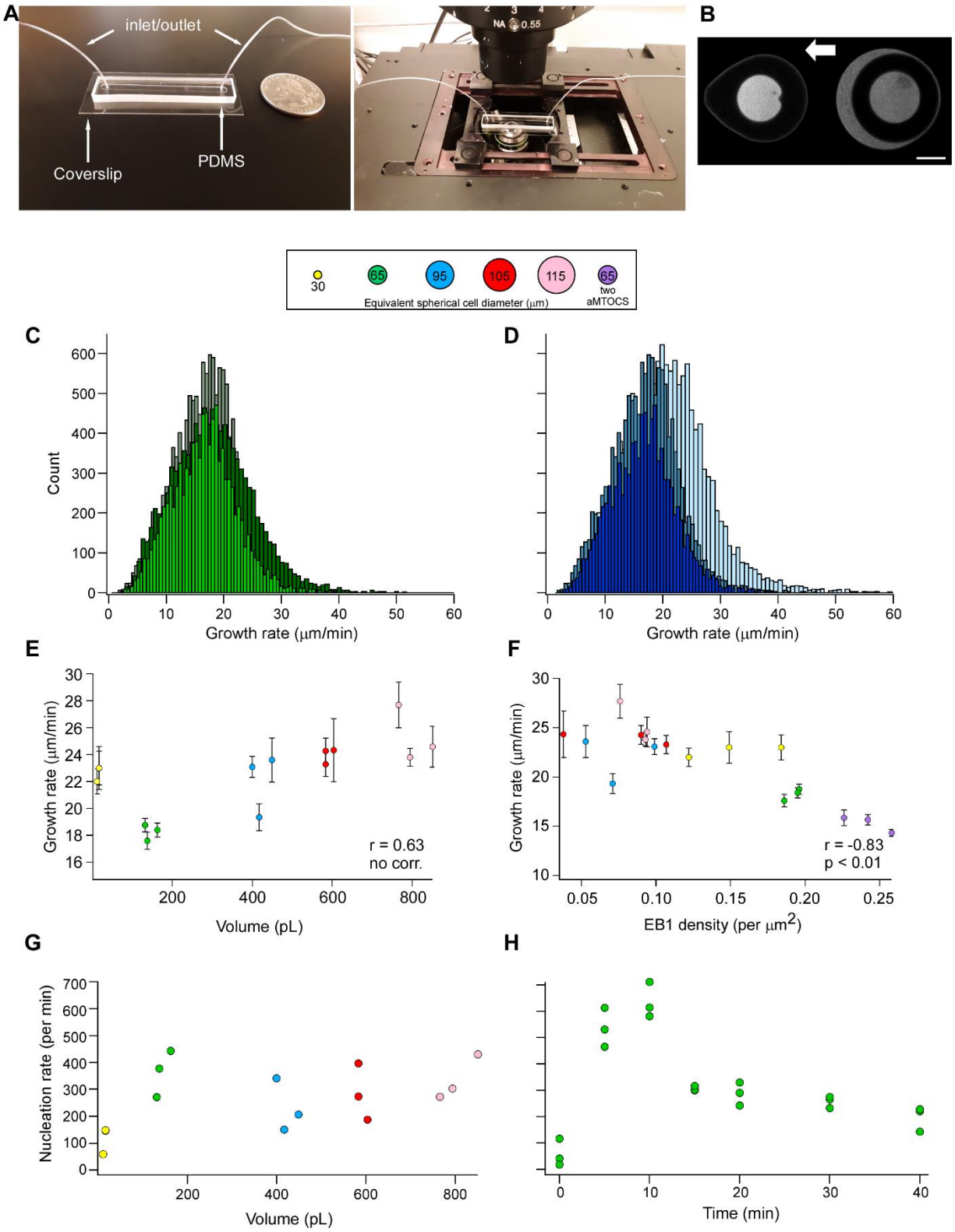

FIgureS1. Experimental design, kymograph analysis, and nucleation rates. Related to Figures 1-3. (A) PDMS microfluidic flow chamber shown with an American quarter dollar for

scale. Rightmost panel shows the same PDMS chamber loaded onto an IX-71 stand for formation of PEGDA micro-enclosures. **(B)** PEGDA micro-enclosures under oil crossflow (direction of oil crossflow is indicated by the white arrow). Fluorescent signal (EB1-GFP) is trapped on the exterior of the micro-enclosure when a circular PEGDA structure (right image) is subjected to oil crossflow**,** whereas the fluorescent signal is contained within tear-drop shaped micro-enclosure (left image; scale bar = 50 μm). **(C)** Microtubule growth rates for the 130 pL micro-enclosures, and **(D)** the 400 pL micro-enclosures displayed as histograms. **(E)** MT growth rates, as determined by manual kymographs, plotted as a function of cytoplasmic volume, and **(F)** EB1 density ($n \geq 30$ kymographs per data point). Error bars equal two SEMs. Pearson correlation coefficient (r) is indicated at the side of each graph and is significant if $p < 0.01$ (the absence of a correlation is indicated otherwise). **(G)** Nucleation rate from the aMTOC as a function volume. The radius of the circle used to detect nucleation rate (see Methods) was set at one fifth the diameter of the micro-enclosure. **(H)** Nucleation rate from the aMTOC as a function of time within a 130 pL micro-enclosure. The results for a circle of radius 20, 25, and 30 μm are shown for each time interval.

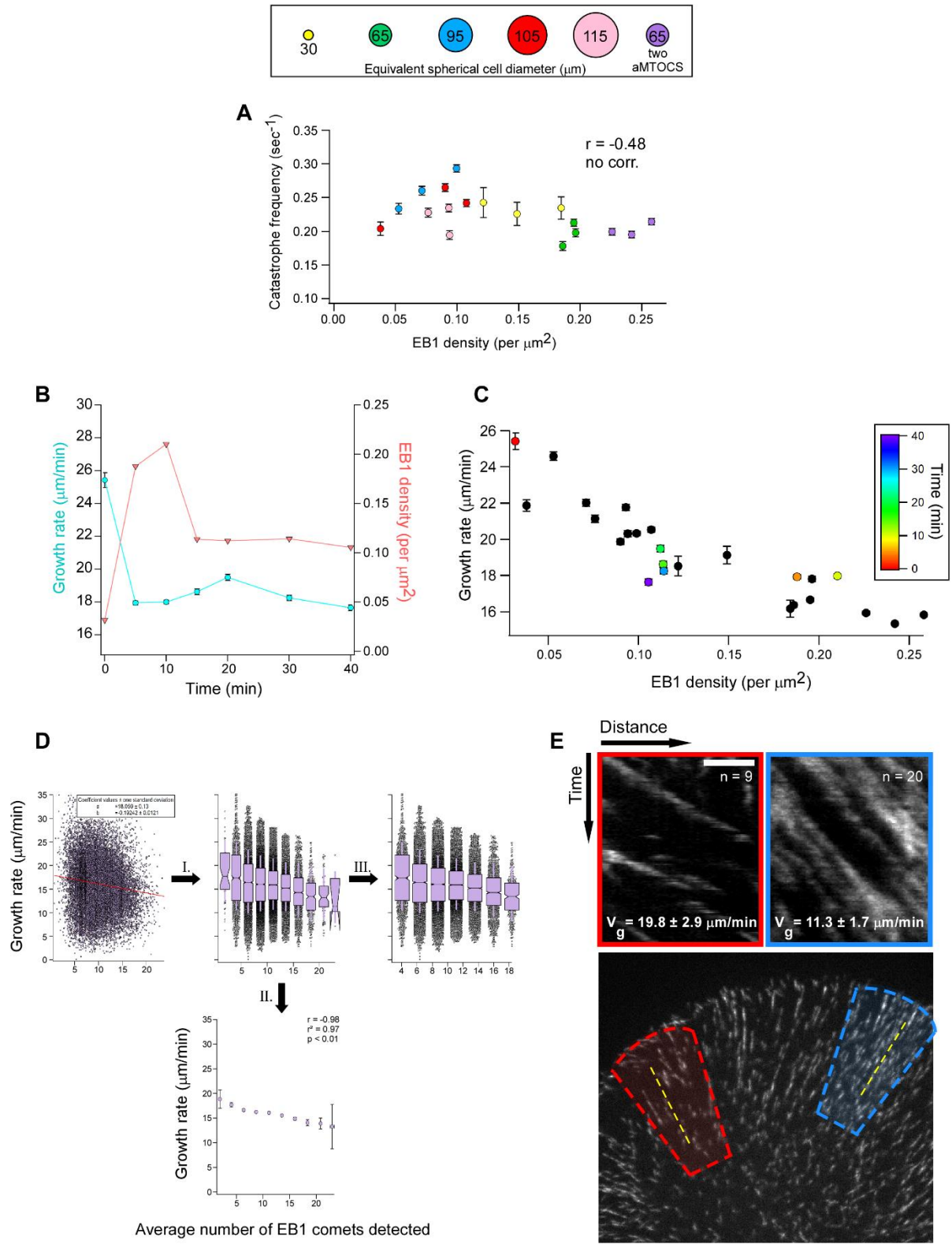

Figure S2. Catastrophe frequency, time evolution of growth rates, and local kymograph analysis. Related to Figures 3 and 4. (A) Microtubule catastrophe frequency plotted as a

function of EB1 density. Error bars equal two SEMs. Pearson correlation coefficient (r) is indicated at the side of each graph and is significant if $p < 0.01$ (the absence of a correlation is indicated otherwise). **(B)** Time development of a 130 pL micro-enclosure, displaying both the MT growth rates and the EB1 density as a function of time. 0 min corresponds to the start of the first image-sequence. **(C)** MT growth rates from a 130 pL micro-enclosure imaged over 40 minutes displayed as a function of EB1 density and overlaid on the plot from Figure 3a. Data points depicted in black represent those taken from Figure 3a. **(D)** Average velocity (i.e., growth rate) for every EB1 comet plotted against its local density (average number of EB1 comets detected in a 3 μm search radius). Each dot corresponds to a single EB1 track (n = 20,481). The slope of the spread was determined using a linear fit, with $y = a + bx$. **(I)** The raw spread from the analysis was subdivided into 10 bins, with each bin consisting of a ~10% increment of the highest local density observed for that search radius. In this example, the highest local density observed was 25 EB1 comets within a 3-μm search radius. As a result, each bin spans a range of approximately 0.1×25, or 2.5 EB1 comets, with each bin centered on the mean local density contained within the bin. **(II)** The mean local density and mean growth rate of each bin was then used to determine Pearson's correlation coefficient (r), Pearson's coefficient of determination (r^2), and the p-value for each local density analysis. All statistical analyses were performed on the entire data set (II). **(III)** Each bin was then plotted as a box plot, with Tukey-style IQRs, whiskers displaying one SD, and notches indicating the 95% confidence interval of the median. For graphical display (Figure 4), those bins containing <1% of the total population (for this example, 205 data points) were removed. **(E)** Representative kymographs from two regions within the same micro-enclosure (bottom-most panel). The yellow lines correspond to the ROI used to generate the example kymographs displayed in the upper-left and upper-right panel. For each region, five non-overlapping ROIs were used to assess the growth rate (displayed in the upper panels) (scale bar = 3 μm).

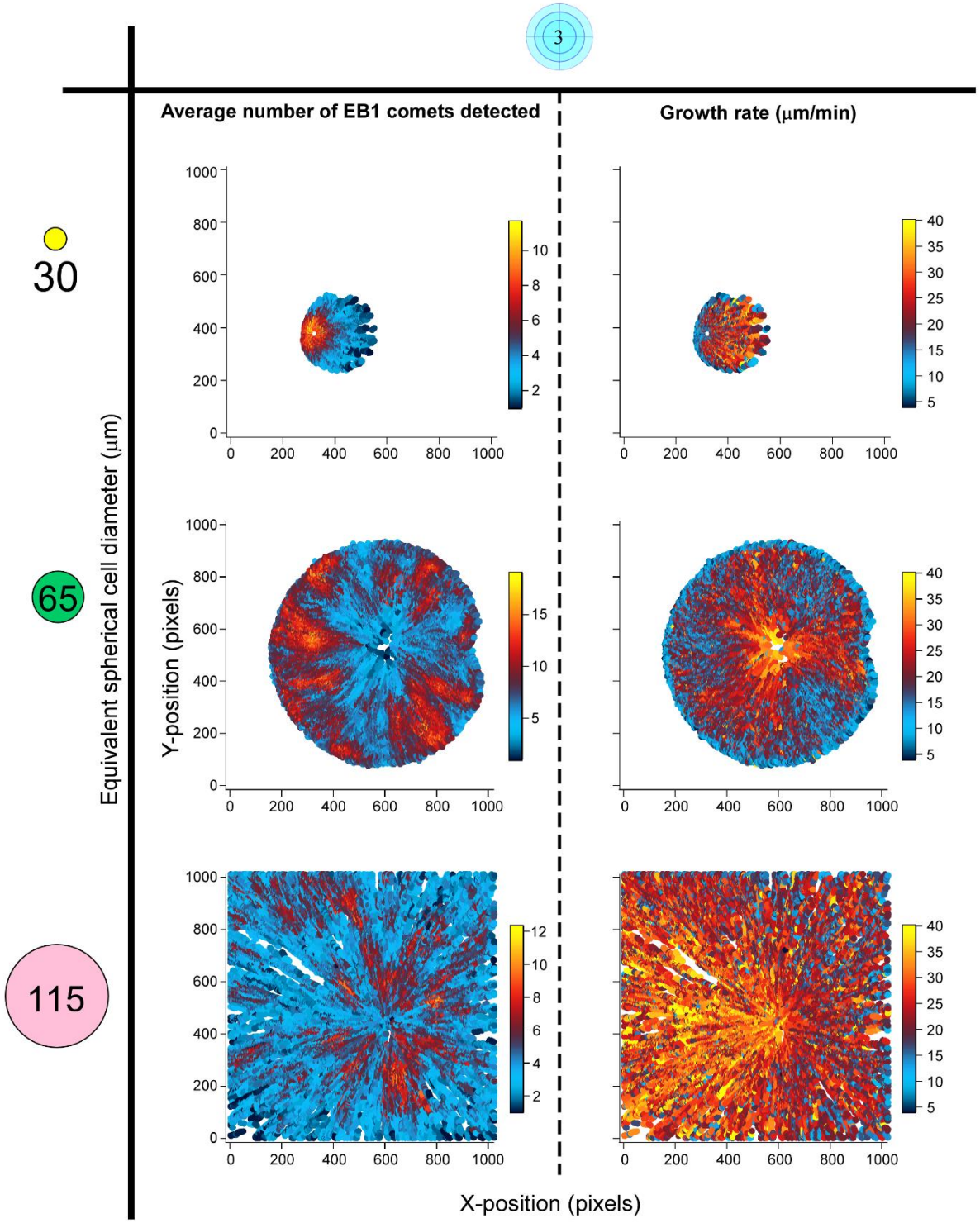

Figure S3. Local EB1 density heat maps for a range of micro-enclosures. Related to Figure 4. The average number of EB1 comets detected within a 3 μm search radius and the average growth rate of each EB1 comet plotted against coordinate position for micro-enclosures of ~11, ~160, and ~800 pL (spherical cells of 30, 65, and 115 μm Ø, respectively).

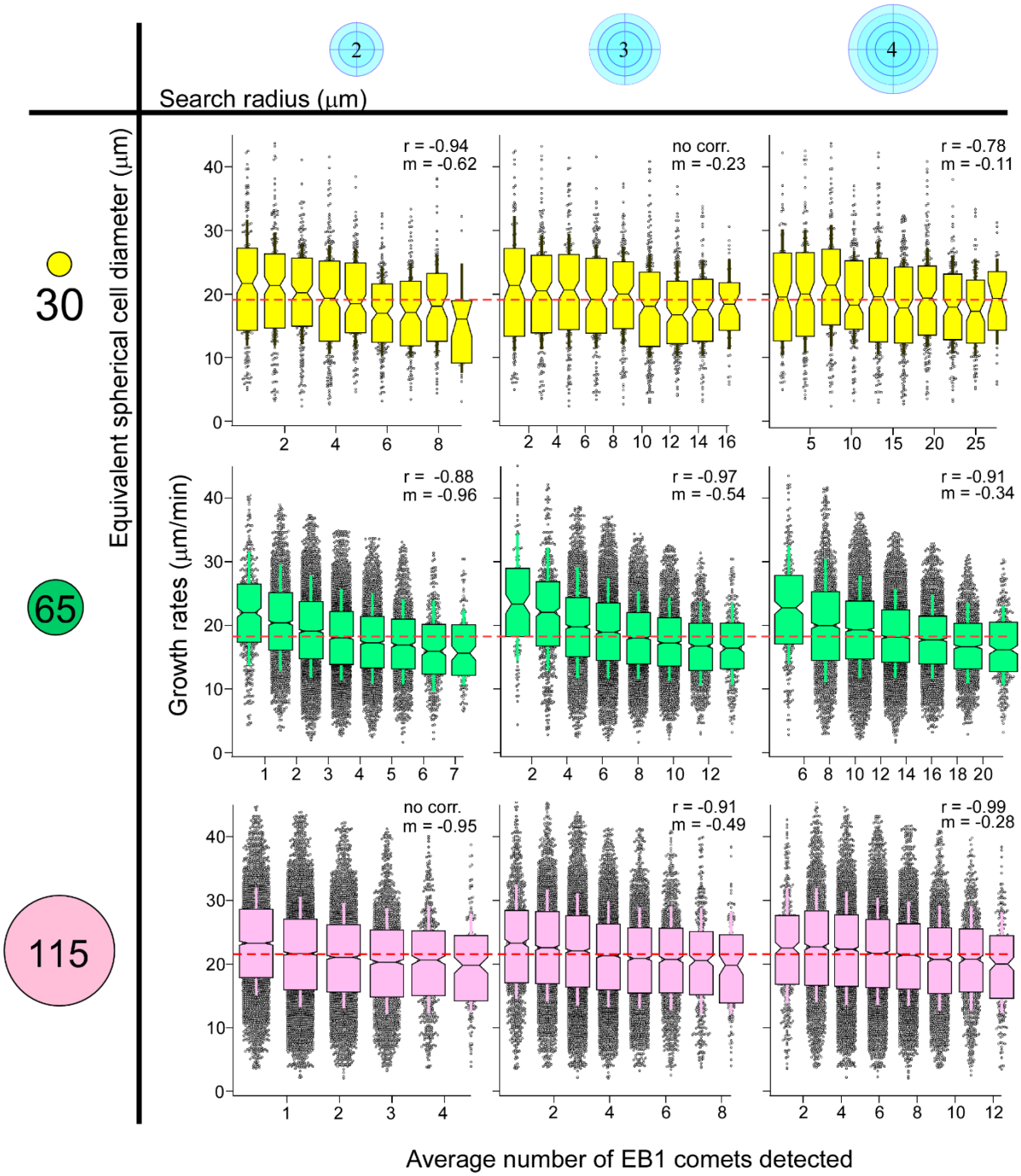

Figure S4. Microtubule growth rates as a function of local EB1 density. Related to Figure 4. Average MT growth rates as a function of local density. The results from three search radii (indicated by blue circles) are shown for micro-enclosures of ~11, ~160, and ~800 pL (spherical cells of 30, 65, and 115 μm Ø, respectively). Dashed red line indicates the mean global growth rate for the system. Box plots are displayed with Tukey-style IQRs, whiskers displaying one SD, and notches indicating the 95% confidence interval of the median. Pearson's correlation

coefficient (r) is displayed at the top of each graph with the slope (m) of the linear fit. Correlations were significant if $p < 0.01$ (the absence of a correlation is indicated otherwise).